ELEKTROTEHNIŠKI VESTNIK 78(5): 257-262, 2011
ENGLISH EDITION

# Detection of the Electrocardiogram Fiducial Points in the Phase Space Using Area Calculation

**Emil Plesnik[1], Olga Malgina[2], Jurij F. Tasič[1], and Matej Zajc[1]**

[1] *Univerza v Ljubljani, Fakulteta za elektrotehniko, Tržaška 25, 1000 Ljubljana, Slovenija*
[2] *Inštitut Jožef Stefan, Jamova 39, 1000 Ljubljana, Slovenija*
*E-pošta: emil.plesnik@fe.uni-lj.si*

**Abstract.** The paper proposes an extension of a known method for heart-beat detection based on ECG reconstruction in a 2D phase space coherent to the delay method to detection of the P-Q-R-S-T characteristic (fiducial) points. The QT Database was used for evaluation and algorithm performance was assessed using sensitivity (Se) and positive predictive value (PPV). Results are 99.19 %, 99.67 % and 94.58 % for Se and 95.02 %, 99.67 % and 94.55 % for PPV for the P points, heartbeats and T points, respectively.

**Keywords:** phase space, phase portrait, ECG signal, fiducial points, digital signal processing

## 1 INTRODUCTION

The goal of the paper is to present an extension of a known method for heart-beat detection based on ECG reconstruction in a 2D phase space to detection of the P-Q-R-S-T characteristic (fiducial). The paper focuses on processing a single-lead ECG signal by means of which information about the cardiovascular system (CVS) functioning is extracted [1, 2].

Phase space based methods for signal processing are well established [3–10]. The paper reviews development of phase space based ECG processing methods for the last two decades [1, 2, 11–21].

ECG signal processing is decisive in diagnosis of cardiac disorders. Most of the clinically relevant information in the ECG signal can be derived from the analysis of the P-Q-R-S-T waves of the cardiac cycle (Fig. 1). Therefore, detection of these characteristic waves is one of the essential tasks in ECG signal processing [22]. For that reason, the development of effective and automated methods for detection of the mentioned waves and heart arrhythmias is of value for long recordings of patients with coronary diseases [23].

Nevertheless, emerging nonmedical applications of the ECG signal also express the need for detection of fiducial points, such as human identification [24] and emotion recognition [25]. The results in [24] show that the features extracted from digitally detected fiducial points are independent of sensor location, invariant to the individual's state of anxiety and unique to an individual and hence, appropriate for human identification. Results in [25] state that ECG features extracted from the fiducial points excellently express the emotion state of an individual with an almost 90 % success rate for sadness and joy.

Automated detection of these characteristic waves has been addressed before [11, 22, 24–32]. The term fiducial (reference) points is a common term for characteristic points which are local maxima or minima of characteristic waves. Different methods have been proposed for detection of the fiducial points in the ECG signal, such as signal derivatives and digital filtering [11, 22], Wavelet Transformation [26, 28, 31], Neural Networks [27], Hidden Markov Models [29], Hilbert Transformation [30], etc.

According to [3] CVS is an example of a nonlinear dynamical system. Because of non-damping oscillations CVS can be treated as a self-sustained oscillator which is not strictly periodic [1, 4]. The knowledge of deterministic dynamical chaos in real dynamical systems (such as CVS) is based on the properties of attractors (phase portraits) serving as the mathematical image of such systems [3].

A phase portrait is a graphical presentation of dynamical-system oscillations in phase space. The method of analyzing oscillations of dynamical systems through phase portraits was introduced in [5]. A phase portrait of a system is a set of paths that represent all of its possible histories. Each point in the phase portrait represents a specific state of the system in time. Analysis of phase portraits of complex oscillations enables assessing topological structures of chaotic attractors and making valuable assumptions for further investigations.

According to [3] a dynamical system, which can be observed experimentally in time and cannot be described by equations, is called a "black box" dynamical system. The entire available information

*Received September 28, 2011*
*Accepted October 24, 2011*

about such a system is contained in the input and output signals only. The output signal is measured experimentally in the form of a one-dimensional time series

$$x_k = x(k*\Delta t),\ k = 1, \ldots, N. \quad (1)$$

The techniques for reconstructing phase portraits of dynamical systems from their scalar time series are introduced in [6] and the mathematical definition of the delay method is given in [7]. This method was also presented in [8], where it was used in modeling of chaotic time series. In the nineties, reconstructing phase portraits from the scalar time series was applied by several authors in processing of electrocardiogram signals [1, 11–13]. Implementations of the method in the field of cardiography continued in the last decade in [2, 14–17].

A phase portrait visualizes the entire ECG record in a single small-size figure thus, simplifying handling with ECG recordings as it removes scrolling longer records in time (Fig. 1) and simultaneously presents several ECG signal characteristics, such as the P-Q-R-S-T waves, of the complete ECG record.

There were also hardware implementations of cardiac abnormalities detectors [18, 19], where the authors describe the method as fast and accurate and highly noise resistant enabling the use in small, portable and wearable wireless devices limited with energy supply and processing power (mobile phones, smartphones, electronic patches, etc.). In both cases, real-time processing of the ECG signals using phase portraits was demonstrated. Furthermore, phase portraits are reported in major EU research projects, such as [33] and [34].

The method of phase portraits was described in detail in [3, 9, 20]. A very informative description of nonlinear time-series analysis of the human ECG is given in [21]. According to the authors, the method of delays determined in [19] is the most simple for phase-portrait reconstruction and therefore most widely used. In fact, most of the authors mentioned in this section have used the delay method in their work. Nevertheless, other methods for phase-portrait reconstruction are also possible, e.g. derivation, integration [2, 10], although rarely used.

## 2 SETUP

The algorithm was evaluated by using the QT Database [35] designed to evaluate algorithms detecting waveform boundaries in ECG. It contains 105 ECG recordings with signals sampled at 250 Hz, each 15 minutes long (containing 225.000 samples). Recordings in the QT Database [35] contain two ECG leads with manually determined waveform boundaries and fiducial points on subsets of heartbeats in each signal. These

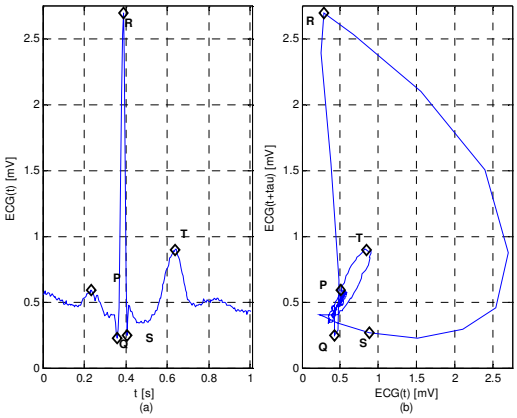


Figure 1: Normal ECG signal segment from the recording sel100 of the QT Database [35] in (a) time space and (b) phase space.

subsets of annotated heartbeats included at least 30 heart beats in each signal record. In all, 3622 QRS complexes, 3193 P points and 3541 T points were annotated in the database.

The algorithm was designed and evaluated in MATLAB® [36].

## 3 METHOD

### *3.1 Characteristics of a normal ECG signal*

The ECG signal is visualization of the electrical cyclic activity of the heart. An ECG signal is captured with electrodes acquiring the body surface potentials and the difference between two electrode readings representing one ECG lead. The standard in medicine cardiac monitoring is the 12-lead ECG [38]. It consists of 12 different ECG leads exposing the heart cyclic activity from 12 different directions. For a complete 12-lead ECG, 10 electrodes need to be placed on specific locations of the body [37]. This paper focuses on a single ECG lead (preferably lead II) proved to be sufficient for phase portrait reconstruction and detection and classification of the ECG signal [1, 2].

A normal ECG cycle of the lead II signal is shown in Fig. 1. It starts with a positive P wave which is a result of the heart atria contraction (depolarization). This is followed by a combination of three waves: a negative Q, a positive R and a negative S. This is called the QRS complex and represents the atria relaxation (repolarization) and ventricular depolarization which happen at the same time. The heart cycle is concluded by a positive T wave representing ventricular repolarization. The amplitudes of these five waves along with time intervals between them are ECG signal characteristics and represent important information about the heart function.

The ECG signal is very diverse and each individual has a unique signal pattern. However, normal ECG signal characteristics are statistically determined and are also valid for lead II in [37].

### *3.2 Phase-space reconstruction – delay method*

In general, as defined by [6] and [7], a phase portrait of a dynamical system, described by a one-dimensional time series of measured scalar values $y(t)$, can be reconstructed in a $k$-dimensional state space. From the time-series signal we can construct an $n$-dimensional signal $\mathbf{Y}(t)$

$$\mathbf{Y}(t) = [y(t), y(t+\tau), \dots, y(t+\tau(n-1))]^T, \quad (2)$$

where $\tau$ is the time delay and $n$ is the mapping dimension of the reconstruction space. The result of the reconstruction process is the phase portrait presented in an $n$-dimensional phase space.

We reconstructed the phase portrait in a 2D ($n$ = 2) phase space ($y(t)$, $y(t + \tau)$). The phase portrait reconstruction is shown in Fig. 1 with a single ECG cycle visualized in time and phase space along with five correlated points in every figure.

The phase portrait – is the end result of the reconstruction procedure – is shown in Fig. 1(b). The amplitude values of the selected ECG signal segment in Fig. 1(a) serve as the abscissa values for Fig. 1(b) and the amplitude values of the delayed signal segment represent the ordinate values for the phase portrait in Fig. 1 (b). Since the space dimension is determined, the shape of the polygons in the phase portrait depends entirely on the choice of delay.

### *3.3 Optimal delay selection*

The QRS complex (combined Q, R and S waves) and the P and T waves cause specific trajectories and shapes in the phase portrait. A number of consecutive points on these trajectories compose polygons. Based on their area size, we can distinguish between the QRS complex and the P and T waves. The following section describes the algorithm for detecting the QRS complexes and the P and T waves. These waves and complexes give rise to three different polygons in the 2D phase portrait of the ECG signal (Fig. 1). The largest and most significant polygon in the phase portrait is the result of the QRS complex, the smaller polygon corresponds to the T wave and the smallest polygon is caused by the P wave.

The size of the polygons corresponds to the amplitudes of specific waves in the ECG signal and to the chosen delay. This means that the QRS complex with the highest amplitude matches the largest polygon. However, the size of the polygons can be further increased by choosing a proper delay value. To allow for a more clear distinction between the characteristic waves, the polygons should be open and maximized in the area size.

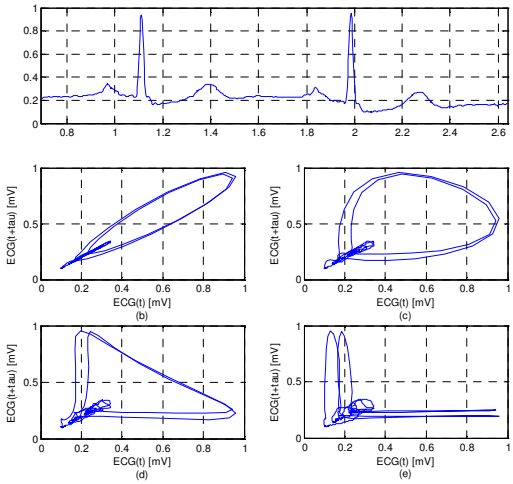


Figure 2: Impact of different delay values on the shape of the phase portrait on an example of two ECG cycles (a): 4 ms (b), 10 ms (c), 20 ms (d) and 40 ms (e).

At small values of $\tau$, the value of $y(t+\tau)$ is near $y(t)$ and the resulting phase portrait is concentrated around the diagonal $y = x$ of the 2D phase space. With increasing $\tau$, the phase portrait diverges from the diagonal until a breaking point, where the phase portrait loses its round shape.

Fig. 2 visualizes the impact of different delay values on the shape of the phase portrait on an example of two ECG cycles (Fig. 2(a)) from the recording sel100 of the QT Database [35]. The time delay for the reconstruction of the phase portrait in Fig. 2(b) is 4 ms, which is considered small since it represents one signal sample. Thus, the resulting phase portrait is concentrated near the diagonal of the phase space. Nevertheless, when the delay is increased, the phase portrait increases in its size and stretches away from the diagonal. Fig. 2(c) shows the phase portrait at the time delay of 10 ms. The increase in the phase-portrait size is evident compared to Fig. 2(b). The phase portrait continues growing in its size together with the delay values to around 20 ms (Fig. 2(d)), when it reaches the breaking point. This means that the phase portraits for the delay values above 20 ms are intersecting and divided into several smaller loops thus, complicating detection of specific points. The algorithm is still effective till the delay values of about 80 ms. An example of such intersected phase portrait is shown in Fig. 2(e) with the delay being 40 ms. According to this visual experience, the optimal delay would be the value just before the breaking point, which is 20 ms.

To confirm this optimal delay, the algorithm was tested on a one minute segment of the ECG signal from recording sel16265 from the QT Database [35]. In the selected minute of the signal there are 67 normal heart beats. The phase portrait was reconstructed according to Section 3.2. Fig. 2 (a) – (h) represents phase portraits

Table 1: Detection of the R waves through phase-portrait area calculation.

| Delay [no. of samples] | No. of detected R waves | PPV = [%] |
|---|---|---|
| 1 (2 – 5 ms) | 67 | 100 |
| 5 (18 – 21 ms) | 67 | 100.0 |
| 8 (30 – 33 ms) | 67 | 100.0 |
| 10 (38 – 41 ms) | 67 | 100.0 |
| 15 (58 – 61 ms) | 67 | 100.0 |
| 18 (70 – 73 ms) | 67 | 100.0 |
| 19 (74 – 77 ms) | 67 | 100.0 |
| 20 (78 – 81 ms) | 68 | 100.0+1.5 |
| 21 (82 – 85 ms) | 75 | 100.0+11.9 |
| 22 (86 – 89 ms) | 95 | 100.0+41.8 |
| 23 (90 – 93 ms) | 113 | 100.0+68.7 |
| 25 (98 – 101 ms) | 130 | 100.0+94.0 |

for the selected signal at different delay values. With the experiment we planned to show the impact of the selected time delay on the algorithm efficiency, hence the time delay was the only variable.

The testing results are shown in Table 1 giving the number and percentage of the detected R waves in the signal (2nd and 3rd column) at various delay values (1st column). The delay values are given as the number of samples and are also calculated in milliseconds. According to Section 2, one sample is taken every four milliseconds.

From the results given in Table 1 we can conclude that the algorithm to be used in detection of the R wave by using area calculation in the phase portrait is works very well till the delay value of 20 samples (approximately 80 milliseconds) and after that at higher delay values its effectiveness decreases very quickly. With the delay of 23 samples (approximately 90 milliseconds), the algorithm fails completely as it detects 46 additional R waves that are not true.

In [18] and [19], 20 milliseconds were chosen as the optimal delay. This is in line with our experiments, which return good results for the delay values between 2 ms and 80 ms. Therefore, we chose the time delay of 20 ms for the experiment presented in this paper.

### *3.4 Detection using area calculation in the phase space*

To determine the fiducial points representing the local maxima or minima of the mentioned waves, we calculated the areas of individual polygons to create the detection function. After selecting the time delay and reconstructing the phase portraits, the characteristic-point detection can proceed by determining the detection function. Elements of the detection function for this method are the area values of the consecutive polygons. The area size of a polygon is calculated by using a plane-geometry equation for the planar non-self-intersecting polygons (3)

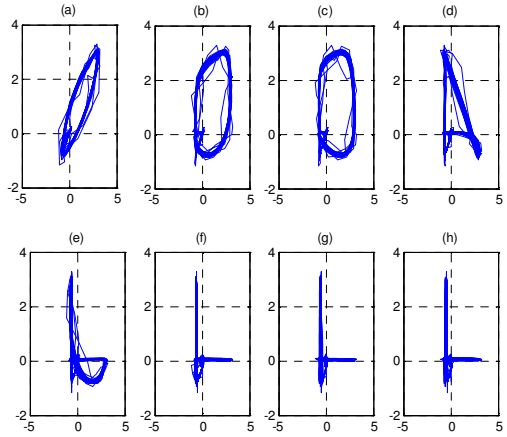


Figure 3: Phase portraits of the ECG signal from the recording sel16265 from the QT Database [35] at different delay values: 5 ms (a), 15 ms (b), 20 ms (c), 30 ms (d), 45 ms (e), 70 ms (f), 85 ms (g) and 100 ms (h). On the x axis of each phase portrait there are amplitude values in millivolts of the non-delayed ECG signal and on the *y* axis there are amplitude values in millivolts of the delayed ECG signal.

$$S=\frac{1}{2}\left(abs\begin{vmatrix}x_1 & x_2\\ y_1 & y_2\end{vmatrix}+abs\begin{vmatrix}x_2 & x_3\\ y_2 & y_3\end{vmatrix}+...+abs\begin{vmatrix}x_{n-1} & x_n\\ y_{n-1} & y_n\end{vmatrix}\right) \quad (3)$$

We consider the absolute values as the orientation of the polygons is not relevant. Parameter *n* in equation (3) denotes the number of samples comprising one area considered for calculation.

Selection of the value of parameter *n* depends on the sampling frequency and QRS complex duration [18]. This means that if the average QRS complex is less than 100 milliseconds, which is 25 data samples at 250 samples per second, none of the polygons comprised of 10 data samples is intersecting. This can be generalized for using different sampling frequencies: the number of sample points comprising the polygons is less than half of the number of sample points representing an average QRS complex of 100 milliseconds. Therefore, in our experiments the number of samples was equal to approximately one third of the QRS complex duration, e.g. from 60 – 120 ms. For example, if an ECG signal is sampled at 250 Hz, it is recommended to take at least 5 - 10 points for polygon description.

Once the detection function is ready the QRS complexes can now be detected by using the threshold function. However, the detected QRS complexes are indicators of a present heart beat and give no information about exact locations of the Q, R and S specific points. Therefore, the next step in the algorithm is to determine exact locations of the R points in the signal.

Locations of the R points are determined by using the detected QRS complex locations and the duration of the normal QRS complex. The algorithm checks for the

Table 2: Specific-point detection results using phase space area calculation.

| | | | | | | Points P | | Points QRS | | Points T | |
|---|---|---|---|---|---|---|---|---|---|---|---|
| annotated points P | detected points P | annotated complexes QRS | detected complexes QRS | annotated points T | detected points T | Se=TP/(TP+FN) [%] | PPV=TP/(TP+FP) [%] | Se=TP/(TP+FN) [%] | PPV=TP/(TP+FP) [%] | Se=TP/(TP+FN) [%] | PPV=TP/(TP+FP) [%] |
| 3193 | 3333 | 3622 | 3622 | 3541 | 3542 | 99.19 | 95.02 | 99.67 | 99.67 | 94.58 | 94.55 |

maxima in a defined time window with the detected QRS complex of the analysed ECG signal positioned as the centre point. The highest maximum in this time window is recognized as the R point. The width of the time window is twice the width of the maximum normal QRS complex, which is 120 milliseconds [37]. Both neighbouring Q and S points are detected as the local minima before (Q point) and after (S point) the R point in the same interval.

Detection of the T points is similar to detection of the R points. Indicators of the T peaks are extracted from the detection function on intervals between the QRS complexes as a local maximum. So, the exact locations of the T points are detected in the signal in the time window around the indicator. The time window is 200 milliseconds wide, which is the maximum value for the T wave [37, 38]. The first fiducial point of the ECG cycle is detected last from the signal according to the known locations of the previously detected fiducial points. The P point is detected as a local maximum in the time window between the Q point and 200 milliseconds before the Q point, which corresponds to the maximum value of the P-R interval [37].

## 4 RESULTS

Results of our experiment for the algorithm using the polygon area calculation in phase portraits for fiducial point detection are given in Table 2. The first, third and fifth column give the total number of the annotated P, QRS and T points in the entire QT Database [35]. The second, fourth and sixth column give the total number of the detected P, QRS and T points, respectively. The last six columns present sensitivity (Se [%]) and positive predictivity (PPV [%]) for the detected P, QRS and T points. The values of parameter Se are 99.19 % for the P points, 99.67 % for the QRS complexes and 94.58 % for the T points. The values for parameter PPV are 95.02 % for the P points, 99.67 for the QRS complexes and 94.55 % for the T points.

## 5 DISCUSSION

Records used in this paper are from the QT Database [35] designed to evaluate algorithms detecting waveform boundaries in ECG. Signals from the QT Database [35] include a broad variety of the QRS and ST-T morphologies. All these variations are representing real clinical conditions.

The standard performance measures, such as sensitivity (Se) and positive predictivity (PPV) are tested for the algorithm for fiducial points detection. Se represents the percentage of the true fiducial points correctly detected by the algorithm and the PPV represents the percentage of fiducial points detections which were in reality true. The Se and PPV tests reflect detection performance for fiducial points detection using phase-space area calculation.

The algorithm using area calculation in the phase space performs well and stable in average for all signals from the database (Table 2). Its performance for QRS detection is comparable with other methods [26, 31, 32]. Efficiency is excellent as it achieves 100 % in all signals but one. The only signal the algorithm failing to detect all the QRS complexes correctly is sel102 containing pacemaker heart beats. In all, 12 QRS complexes were false detected (detected as FP) in the signal sel102 and the entire QT Database [35].

Compared to methods from [31, 32], there is room for improvement in the performance of the algorithm for P and T point detection, which is slightly lower because of false detections due to the missing waves and inverted or biphasic waves, occurring due to the abnormalities of the heart function, such as atrial block, etc. Out of the 3333 detected P points there are 166 false detections (FP), which is the reason for lower PPV. On the other hand, Se is over 99 % because only 26 P points were missed (FN). This means that the algorithm has a good detection rate for the P points, nevertheless it is sensitive for the missing P waves in abnormal events in the ECG signals, such as atrial blocks. In addition, there were 3542 detected T points out of which 193 were false detections (FP) and consequently 192 missed T points (FN). This results in lower Se and PPV values being mainly due to the biphasic T waves. The algorithm determined the peak of the positive part of a biphasic wave as the T point, while the manual annotation was set in the middle of the wave.

## 6 CONCLUSION

The paper proposes an extension of an established algorithm used in detection of heart beats with area calculation of phase portrait polygons for fiducial points detection in ECG signals. Testing on the QT Database [35] gives comparable results to the state-of-the-art.

## ACKNOWLEDGEMENT

This work was supported by ARRS under the P2-0246 Scientific Program.

## REFERENCES

[1] P. Saparin, M. Zaks, J. Kurths, A. Voss, and V. Anishchenko, "Reconstruction and structure of electrocardiogram phase portraits," *Phys rev E,* vol. 54, no. 1, pp. 737–742, Jul. 1996.

[2] G. Dori, Y. Denekamp, S. Fishman, A. Rosenthal, B. S. Lewis, and H. Bitterman, "Evaluation of the phase-plane ECG as a technique for detecting acute coronary occlusion," *Int J Cardiol*, vol. 84, pp. 161–170, 2002.

[3] V. S. Anishchenko, V. Astakhov, A. Neiman, T. Vadivasova, and L. Schimansky-Geier, *Nonlinear dynamics of chaotic and stochastic systems: tutorial and modern developments*. Springer Verlag, 2002.

[4] A. Babloyantz and A. Destexhe, "Is the normal heart a periodic oscillator?," *Biol Cybern*, vol. 58, no. 3, pp. 203–211, 1988.

[5] A. A. Andronov and C. E. Chaikin, *Theory of oscillations*. Princeton University Press, 1949.

[6] N. H. Packard, J. P. Crutchfield, J. D. Farmer, and R. S. Shaw, "Geometry from a time series," *Phys Rev Lett*, vol. 45, no. 9, pp. 712–716, 1980.

[7] F. Takens, "Detecting strange attractors in turbulence," *Dynamical systems and turbulence,* pp. 366–381, 1981.

[8] M. Casdagli et al., "Nonlinear modelling of chaotic time series: Theory and aplications," in *Applied Chaos*, J. H. Kim and J. Stringer, Eds. John Wiley & Sons, Inc., 1992, pp. 335–381.

[9] H. D. I. Abarbanel, *Analysis of Observed Chaotic Data*, vol. 39. Springer, 1997.

[10] N. B. Janson, A. N. Pavlov, and V. S. Anishchenko, "One method for restoring inhomogeneous attractors," *Int J Bifurcat Chaos*, vol. 8, no. 4, pp. 825–833, 1998.

[11] A. L. Goldberger, "Fractal mechanisms in the electrophysiology of the heart," *IEEE Eng Med Biol Mag*, no. June, pp. 47–52, 1992.

[12] X. S. Zhang, Y. S. Zhu, and X. J. Zhang, "New approach to studies on ECG dynamics: extraction and analyses of QRS complex irregularity time series.," *Med Biol Eng Comput*, vol. 35, no. 5, pp. 467–73, Sep. 1997.

[13] M. Richter, T. Schreiber, and D. T. Kaplan, "Fetal ECG extraction with nonlinear state-space projections.," *IEEE Trans Biomed Eng*, vol. 45, no. 1, pp. 133–7, Jan. 1998.

[14] W. El-Atabany, A. B. . Youssef, and Y. M. Kadah, "Identification and classification of ECG abnormalities using recurrence quantification analysis," in *2nd Cairo Int. Biomed. Eng. Conf.*, 2004.

[15] K. Noponen, J. Kortelainen, and T. Seppänen, "Invariant trajectory classification of dynamical systems with a case study on ECG," *Pattern Recogn*, vol. 42, no. 9, pp. 1832–1844, Sep. 2009.

[16] N. Srinivasan, M. T. Wong, and S. M. Krishnan, "A new phase space analysis algorithm for cardiac arrhythmia detection," *Proc. of the 25th Annu. Int. Conf. of the IEEE EMBS*, pp. 82–85, 2003.

[17] R. Rohani Sarvestani, R. Boostani, and M. Roopaei, "VT and VF classification using trajectory analysis," *Nonlinear Anal Theor Meth Appl*, vol. 71, no. 12, p. e55–e61, Dec. 2009.

[18] J.-W. Lee, K.-S. Kim, B. Lee, B. Lee, and M.-H. Lee, "A Real Time QRS Detection Using Delay-Coordinate Mapping for the Microcontroller Implementation," *Ann Biomed Eng*, vol. 30, no. 9, pp. 1140–1151, Oct. 2002.

[19] M. Cvikl, F. Jager, and A. Zemva, "Hardware Implementation of a Modified Delay-Coordinate Mapping-Based QRS Complex Detection Algorithm," *EURASIP J Adv Sig Pr*, vol. 2007, pp. 1–14, 2007.

[20] U. R. Acharya, S. M. Krishnan, J. A. . Spaan, J. S. Suri, and S. (Service Ligne), *Advances in cardiac signal processing*. Springer-Verlag Berlin Heidelberg, 2007.

[21] M. Perc, "Nonlinear time series analysis of the human electrocardiogram," *Eur J Phys*, vol. 26, no. 5, pp. 757–768, Sep. 2005.

[22] Y. Sun, K. L. Chan, and S. M. Krishnan, "Characteristic wave detection in ECG signal using morphological transform.," *BMC cardiovasc Disord*, vol. 5, p. 28, Jan. 2005.

[23] S. Z. Mahmoodabadi, A. Ahmadian, M. Abolhasani, P. Babyn, and J. Alirezaie, "A fast expert system for electrocardiogram arrhythmia detection," *Expet Syst*, vol. 27, no. 3, pp. 180–200, Jul. 2010.

[24] S. A. Israel, J. M. Irvine, A. Cheng, M. D. Wiederhold, and B. K. Wiederhold, "ECG to identify individuals," *Pattern Recogn*, vol. 38, no. 1, pp. 133–142, Jan. 2005.

[25] Y. Xu, G. Liu, M. Hao, W. Wen, and X. Huang, "Analysis of affective ECG signals toward emotion recognition," *J Electron (China)*, vol. 27, no. 1, pp. 8–14, May 2010.

[26] C. Li and C. Zheng, "Detection of ECG characteristic points using wavelet transforms," *IEEE Trans Biomed Eng*, vol. 42, no. 1, pp. 21–28, 1995.

[27] S. Mohsin, "Unsupervised learning based feature points detection in ECG," in *Proc. of the 8th WSEAS Int. Conf. on Systems Theory and Scientific Computation*, Rhodes, Greece, 2008, pp. 157–160.

[28] O. Sayadi and M. B. Shamsollahi, "Model-based fiducial points extraction for baseline wandered electrocardiograms," *IEEE Trans. Biomed. Eng.*, vol. 55, no. 1, pp. 347–51, Jan. 2008.

[29] S. Graja and J. M. Boucher, "Hidden Markov tree model applied to ECG delineation," *IEEE Trans. Instrum. and Meas.*, vol. 54, no. 6, pp. 2163–2168, 2005.

[30] D. Benitez, P. a Gaydecki, a Zaidi, and a P. Fitzpatrick, "The use of the Hilbert transform in ECG signal analysis.," *Comput Biol Med*, vol. 31, no. 5, pp. 399–406, Sep. 2001.

[31] A. Ghaffari, M. R. Homaeinezhad, M. Akraminia, M. Atarod, and M. Daevaeiha, "A robust wavelet-based multi-lead electrocardiogram delineation algorithm.," *Med Eng Phys*, vol. 31, no. 10, pp. 1219–27, Dec. 2009.

[32] A. Martínez, R. Alcaraz, and J. J. Rieta, "Application of the phasor transform for automatic delineation of single-lead ECG fiducial points," *Physiol Meas*, vol. 31, no. 11, pp. 1467–85, Nov. 2010.

[33] "MyHeart project." [Online]. Available: http://www.hitech-projects.com/euprojects/myheart/.

[34] "HeartCycle Project." [Online]. Available: http://www.heartcycle.eu/.

[35] "Physionet." [Online]. Available: http://www.physionet.org/.

[36] *MATLAB*. Natick, MA: The Mathworks Inc., 2011.

[37] P. Kumar and M. Clark, *Clinical Medicine*, 7th ed. Elsevier, 2009.

[38] C. Haarmark et al., "Reference values of electrocardiogram repolarization variables in a healthy population," *J Electrocardiol*, vol. 43, no. 1, pp. 31–39, 2010.

**Emil Plesnik** is currently working towards his Ph.D. degree in electrical engineering at the UL-FE in the field of signal processing and wireless sensor networks.

**Olga Malgina** is currently working as a young researcher at the Institute Jožef Stefan Institute in Ljubljana, Slovenia. Her research interests include image and signal processing.

**Jurij F. Tasič** is head of the Laboratory for digital signal processing at the UL-FE. His research interests include signal and image processing and telemedicine applications.

**Matej Zajc** is an assistant professor at the UL-FE. His research interests include signal processing, digital communications and interactive multimedia applications.